

Many-body effects in transport through open systems: pinning of resonant levels

S. Ihnatsenka and I. V. Zozoulenko

*Solid State Electronics, Department of Science and Technology (ITN),
Linköping University, 60174 Norrköping, Sweden*

M. Willander

*Solid State Electronics, Department of Science and Technology (ITN),
Linköping University, 60174 Norrköping, Sweden and
Department of Physics, Göteborg University, 412 96 Göteborg, Sweden*

(Dated: April 26, 2018)

The role of electron-electron interaction in transport properties of open quantum dots is studied. The self-consistent full quantum mechanical magnetotransport calculations within the Hartree, Density Functional Theory and Thomas-Fermi approximations were performed where a whole device, including the semi-infinite leads, is treated on the same footing (i.e. the electron-electron interaction is accounted for both in the leads as well as in the dot region). The main finding of the present paper is the effect of pinning of the resonant levels to the Fermi energy due to the enhanced screening. Our results represent a significant departure from a conventional picture where a variation of external parameters (such as a gate voltage, magnetic field, etc.) causes the successive dot states to sweep past the Fermi level in a linear fashion. We instead demonstrate highly nonlinear behavior of the resonant levels in the vicinity of the Fermi energy. The pinning of the resonant levels in open quantum dots leads to the broadening of the conduction oscillations in comparison to the one electron picture. The effect of pinning becomes much more pronounced in the presence of the perpendicular magnetic field. This can be attributed to the enhanced screening efficiency because of the increased localization of the wave function. The strong pinning of the resonant energy levels in the presence of magnetic field can have a profound effect on transport properties of various devices operating in the edge state transport regime. We also critically examine an approximation often used in transport calculations where an inherently open system is replaced by a corresponding closed one.

PACS numbers: 73.23.Ad, 73.63.Nm, 73.21.La, 72.15.Gd

I. INTRODUCTION

A transport regime where a sub-micron lateral structure is strongly coupled to electron reservoirs (leads) is usually referred to as an open one^{1,2}. This transport regime can be realized in quantum wires, dot and antidot structures typically fabricated using a split-gate or related techniques. Such the techniques allow one to obtain devices with desired and variable geometry and parameters such as an electron density and lead openings. The quantum dot operates in an open regime when the gate voltage sets up two quantum point contacts (QPCs) at the entrance and exit of the dot such that they transmit one or more channels (i.e. the conductance of an individual QPC, $G_{QPC} \gtrsim \frac{2e^2}{h}$). In this regime electrons can freely enter and exit the dot, such that the electron number inside the dot is not integer and the chemical potential throughout the whole device in the linear response regime is constant. [Opposite regime emerges when the point contacts are nearly pinched off and is referred to as a Coulomb blockade^{2,3}. In this case the electron number in the dot is quantized and the chemical potential inside the dot is different from that one in the leads]. During the last decade the open quantum dots have received a significant attention providing many important insights into areas such as quantum interference, chaos, decoherence, localization and many others¹. Earlier transport

experiments have been mainly devoted to the dots with hundreds or even thousands electrons. Only recently it has become possible to reduce occupancy down to only a few or even one electron^{4,5}.

Electron-electron interaction is known to have great impact on transport in quantum dots with such pronounced examples as Coulomb blockade³ or Kondo effect⁶. A description of the quantum transport in quantum dots is often based on model Hamiltonians containing phenomenological parameters such as coupling strengths or charging constants^{7,8,9}. In many cases it is not always straightforward to relate quantitatively the above parameters to the physical processes they represent in the real system and sometimes it is not even obvious whether a model description is sufficient to capture the essential physics. At the same time, it is now becomes well recognized that a detailed understanding and interpretation of the experiment might require a quantitative microscopical modelling of the system at hand free from phenomenological parameters and not relying on model Hamiltonians which validity is poorly controlled. The importance of such the modelling can be illustrated by examples including the quantitative description of the compressible/incompressible strips in magnetic field at the edges of the two-dimensional electron gas¹⁰ or explanation of the Hund rule observed in few-electron quantum dots¹¹, just to name a few.

The purpose of the present paper is twofold. First, we develop an approach aimed on full quantum mechanical many-body transport calculations in open systems that starts from the lithographical layout of the device and does not include phenomenological parameters such as coupling strengths, charging constants etc. The whole device, including semi-infinite leads, is treated on the same footing (i.e. the electron-electron interaction is accounted for both in the leads as well as in the dot region). Using the recursive Green's function technique we self-consistently compute the scattering solutions of the two-dimensional Schrödinger equation in magnetic field¹². Following the parametrization for the exchange and correlation energy functionals of Tanatar and Ceperley¹³ the electron-electron interaction is incorporated within the density functional theory (DFT) in the local density approximation^{11,14}. The validity of the DFT approximation is supported by the excellent agreement with the exact diagonalization and variational Monte Carlo calculations performed for few-electron systems¹⁵, as well as by the good quantitative correspondence between the experiment and the DFT calculations for the magnetoconductance of quantum wires¹⁶. Our approach thus accounts for the quantum mechanics nature of the scattering states and the resonant levels as well as for the exchange and correlation beyond the Hartree approximation. At the same time, it accurately describes the global electrostatic and the screening in the dots as well as in the leads.

The second aim of the present paper is to revise the role of the electron-electron interaction in transport properties of open quantum dots. It is widely believed that in open transport regime (as opposed to the Coulomb blockade or Kondo regime), the electron-electron interaction plays only a minor role. The main finding of the present paper is the effect of pinning of the resonant levels to the Fermi energy due to the enhanced screening. Our results represent a significant departure from a conventional picture adopted in most model Hamiltonians as well as in more sophisticated numerical calculations where a variation of external parameters (such as a gate voltage, magnetic field, etc.) causes the successive dot states to sweep past the Fermi level in a linear fashion. We instead demonstrate highly nonlinear behavior of the resonant levels in the vicinity of the Fermi energy. One of the observable consequence of this effect is smearing of the conductance fluctuations. We also show that the resonant level pinning becomes especially pronounced in magnetic field. Thus, accounting for this effect might be important for the interpretation of the magnetotransport experiment in open structures, including e.g. recent studies of the electronic Mach-Zehnder interferometer¹⁷ and the Laughlin quasiparticle interferometer¹⁸, structures designed to test the realization of the topological quantum computing¹⁹, antidot structures^{20,21,22} and others. It should be also noted that the quantum dot structures demonstrating Kondo effect fall into the semi-open transport regime such that accounting for effect of the

nonlinear screening leading to the resonant level pinning might be essential for the interpretation of the experiments in this regime as well.

The paper is organized as follow. Section II presents the model and the Hamiltonian of the system at hand. In Sec. III the numerical method for the self-consistent calculation of the magnetoconductance is described. Computational results are presented and discussed in Sec. IV, and conclusions are given in Sec. V.

II. MODEL

We consider an open quantum dot attached to semi-infinite leads (electron reservoirs) in a perpendicular magnetic field B . A schematic layout of the device is illustrated in Fig. 1(a). Charge carriers originating from a fully ionized donor layer form the two-dimensional electron gas (2DEG) which is buried inside a substrate at the GaAs/Al_xGa_{1-x}As heterointerface situated at the distance b from the surface. Metallic gates placed on the top of the heterostructure define the dot and the leads on the depth of the 2DEG (Figs. 1 (a),(b)).

The Hamiltonian of the whole system (the dot + the leads) can be written in the form

$$H = H_0 + V(\mathbf{r}) \quad (1)$$

where H_0 is the kinetic energy in the Landau gauge, $\mathbf{A} = (-By, 0, 0)$,

$$H_0 = -\frac{\hbar^2}{2m^*} \left\{ \left(\frac{\partial}{\partial x} - \frac{eiBy}{\hbar} \right)^2 + \frac{\partial^2}{\partial y^2} \right\}, \quad (2)$$

$\mathbf{r} = (x, y)$, $m^* = 0.067m_e$ is the GaAs effective mass. The total confining potential within the framework of the density functional theory is the sum of the electrostatic confinement potential, the Hartree potential, and the exchange-correlation potential

$$V(\mathbf{r}) = V_{conf}(\mathbf{r}) + V_H(\mathbf{r}) + V_{xc}(\mathbf{r}). \quad (3)$$

The electrostatic confinement $V_{conf}(\mathbf{r}) = V_{gates}(\mathbf{r}) + V_{donors} + V_{Schottky}$ includes contributions respectively from the top gates, the donor layer and the Schottky barrier. The explicit expressions for the potentials $V_{gates}(\mathbf{r})$ and V_{donors} are given in respectively Ref. 23 and Ref. 24; the Schottky barrier is chosen to be $V_{Schottky} = 0.8$ eV. The Hartree potential is written in a standard form

$$V_H(\mathbf{r}) = \frac{e^2}{4\pi\epsilon_0\epsilon_r} \int d\mathbf{r}' n(\mathbf{r}') \left(\frac{1}{|\mathbf{r} - \mathbf{r}'|} - \frac{1}{\sqrt{|\mathbf{r} - \mathbf{r}'|^2 + 4b^2}} \right), \quad (4)$$

where $n(\mathbf{r})$ is the electron density and the second term describes the mirror charges placed at the distance of b from the surface, $n(\mathbf{r})$ is the electron density, $\epsilon_r = 12.9$ is the dielectric constant of GaAs, and the integration is performed over the whole device area including the semi-infinite leads.

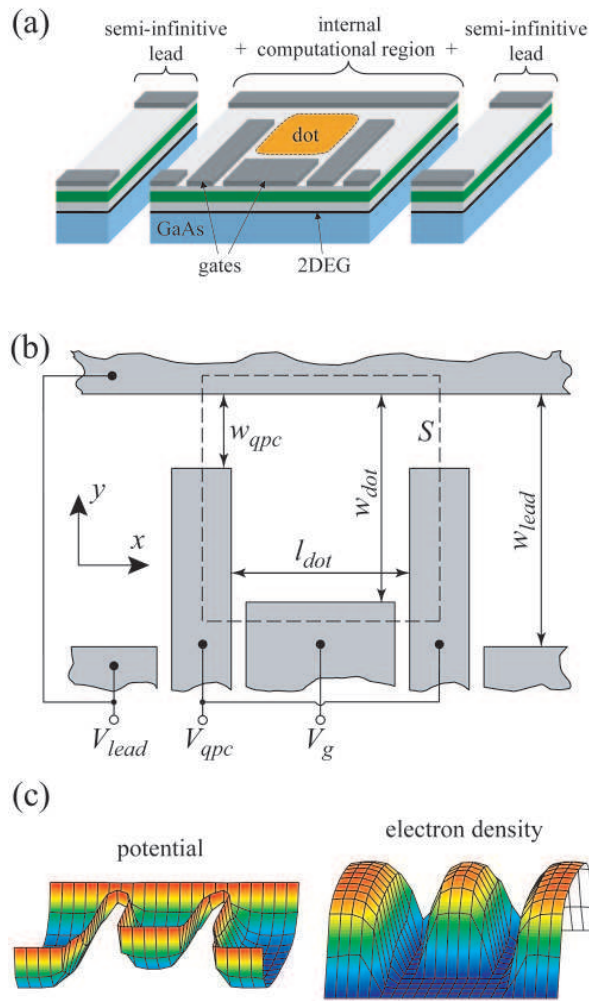


FIG. 1: (color online) (a) Structure of an open quantum dot. The internal region is attached to two semi-infinite quantum wires which serve as the electron reservoirs. (b) The layout of the gates defining the dot. The dashed line defines the area S of the quantum dot used to calculate a number of electrons in it. (c) Representative calculated the self-consistent potential and the electron density.

The last term in the total confining potential (3) is the exchange and correlation potential $V_{xc}[n(\mathbf{r})] = V_x[n(\mathbf{r})] + V_c[n(\mathbf{r})]$ which is the functional of the electron density. In the local density approximation it is given by a functional derivative¹⁴

$$V_{xc} = \frac{d}{dn} \{n\epsilon_{xc}(n)\}. \quad (5)$$

For ϵ_{xc} we have used the parametrization of Tanatar and Ceperley¹³ for the case of spin degenerate electrons. In particular, for the exchange potential this parametrization gives $V_x[n(\mathbf{r})] = -\frac{e^2}{\epsilon_0\epsilon_r\pi^{3/2}}\sqrt{n(\mathbf{r})/2}$. Note that setting $V_{xc}(\mathbf{r}) = 0$ in Eq. (3) we reduce our approach to the standard Hartree approximation.

To outline the role of quantum mechanical effects in the electron-electron interaction in open quantum dots

we also consider the Thomas-Fermi (TF) approximation. In this approximation the kinetic energy is related to the electron density¹⁴, $H_0 = \frac{\pi\hbar^2}{m^*}n(\mathbf{r})$. The self-consistent electron density is thus obtained from the solution of the equation

$$\frac{\pi\hbar^2}{m^*}n(x,y) + V_{conf}(r) + V_H(r) = E_F. \quad (6)$$

The electron density and the total confining potential calculated within the TF approximation do not capture quantum-mechanical quantization of the electron motion. The utilization of the TF approximation for the modelling of the magnetotransport in open system is therefore conceptually equivalent to a one-electron approach. The difference between these approaches is the shape of the total confining potential: in one-electron transport simulations one typically starts with a model hard-wall confinement, whereas the TF approximation gives a rather smooth potential which represents a good approximation to the actual confinement.

III. METHOD

The magnetoconductance through the quantum dot in the linear response regime is given by the Landauer formula²⁵

$$G = -\frac{2e^2}{h} \int dE T(E) \frac{\partial f_{FD}(E - E_F)}{\partial E}, \quad (7)$$

where $T(E)$ is the total transmission coefficient, $f_{FD}(E - E_F)$ is the Fermi-Dirac distribution function and E_F is the Fermi energy. In order to calculate $T(E)$ in perpendicular magnetic field we utilize the recursive Greens function technique in the hybrid energy-space representation¹². We discretize Eq. (1) and introduce the tight-binding Hamiltonian (with lattice constant $a = 4$ nm), where the perpendicular magnetic field is included in a form of the Peierl's substitution²⁵. The retarded Green's function is introduced in a standard way²⁵,

$$\mathcal{G} = (E - H + i\eta)^{-1}. \quad (8)$$

The Green's function in the real space representation, $\mathcal{G}(\mathbf{r}, \mathbf{r}, E)$, provides an information about the electron density at the site \mathbf{r} ,²⁵

$$n(\mathbf{r}) = -\frac{1}{\pi} \Im \int dE \mathcal{G}(\mathbf{r}, \mathbf{r}, E) f(E - E_F). \quad (9)$$

Note that $\mathcal{G}(\mathbf{r}, \mathbf{r}, E)$ is a rapidly varying function of energy. As a result, a direct integration along the real axis in Eq. (9) is rather ineffective as its numerical accuracy is not sufficient to achieve convergence of the self-consistent electron density. Because of this, we transform the integration contour into the complex plane $\Im[E] > 0$, where the Green's function is much more smoother. Note that all poles of the retarded Green's function are in the lower

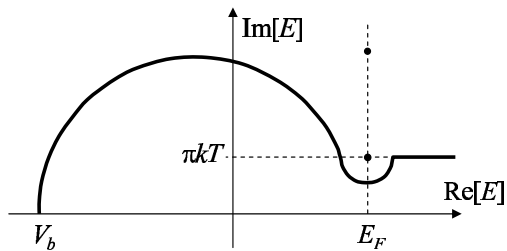


FIG. 2: A typical integration contour used in the calculation of integral (9). Dots indicate the poles of the Fermi-Dirac distribution function in the upper complex plane at $\Re[E] = E_F$, $\Im[E] = (2m + 1)\pi kT$, $m = 0, 1, 2, \dots$. V_b is the bottom of the conduction band in the leads (the lowest potential in the system).

half-plane $\Im[E] < 0$. A typical contour used in the integration avoiding poles of the Fermi-Dirac function is shown in Fig. 2.

In order to calculate the Green's function of the whole system (dot + leads) we divide the system into three parts, the internal computational region and two semi-infinite leads as shown in Fig. 1 (a). Note that the internal region incorporates not only the dot, but also the straight segments including a part of the leads. We place the semi-infinite leads sufficiently far away from the dot where the total self-consistent potential and the electron density do not change along the leads (i.e. the electron density and the potential in the leads are not affected by the internal region, such that the leads can be considered as uniform quantum wires.). This allows us to calculate the total potential and the electron density in the lead regions using the technique developed in Ref. 26 for an infinite homogeneous channel in the perpendicular magnetic field. The Green's function in the internal region is calculated using the standard recursive Green's function technique. The total Green's function for the whole system is calculated by linking with the help of the Dyson equation the surface Greens function for the semi-infinite leads (with the self-consistent potential calculated using the technique of Ref. 26) and the Green's function of the internal region.

All the calculations described above are performed self-consistently in an iterative way until a converged solution for the electron density and potential (and hence for the total Green's function) is obtained. Having calculated the total self-consistent Green's function, the scattering problem is solved where the scattering states in the leads (both propagating and evanescent) are obtained using the Green's function technique of Ref. 26 (The equation for the calculation of the transmission and reflection coefficients using the Green's function in the presence of the magnetic field is derived in Ref. 12).

Having calculated the Green's function of the internal region and the wave function in the leads we can recover the wave function $\psi(\mathbf{r}, E)$ inside the internal region. For visualization of the wave function inside the dot we in-

clude the effect of the finite temperature as follows,

$$|\Psi(\mathbf{r})|^2 = - \int dE |\psi(\mathbf{r}, E)|^2 \frac{\partial f_{FD}(E - E_F)}{\partial E}. \quad (10)$$

In order to find the DOS inside the quantum dot²⁵ we perform integration over the dot area S defined in Fig. 1(b),

$$\text{DOS}(E) = -\frac{1}{\pi} \Im \int_S d\mathbf{r} \mathcal{G}(\mathbf{r}, \mathbf{r}, E). \quad (11)$$

Note that a many-body approach conceptually similar to ours for calculation of the quantum transport in an open dot was developed in Ref. 27 for the case of zero magnetic field. The magnetic field was included in the dot region in the transport calculations presented in Ref. 28 where, however, the leads were considered as non-interacting.

As we mentioned in the previous section, we also employ the TF approximation for the calculation of the magnetotransport through the quantum dot. This calculation is done by the same method as described above, with the only difference that the self-consistent electron densities in the internal region and in the semi-infinite leads are calculated from the semi-classical FT equation (6), as opposed to Eq. (9) that relates the electron density to the quantum mechanical Green's function.

The self-consistent solution in quantum transport or electronic structure calculations is often found using a "simple mixing" method, when on each $m + 1$ iteration step a small part of a new potential is mixed with the old one (from the previous iteration step), $V_{m+1} = (1 - \epsilon)V_m + \epsilon V_{m+1}$, ϵ being a small constant, $\sim 0.1 - 0.01$. It is typically needed $\sim 200 - 2000$ iteration steps to achieve our convergence criterium

$$\frac{|n^{m+1} - n^m|}{n^{m+1} + n^m} < 10^{-5}, \quad (12)$$

where $n^m = \int n^m(\mathbf{r}) dy$ is the electron density in the dot on m -th iteration step. In order to improve the convergence we employ the modified Broyden's second method²⁹ which allows us to reduce drastically the number of iteration steps to $\sim 15 - 40$. An input charge density n_{in}^{m+1} for $m + 1$ iteration is constructed from the sets of input and output densities (n_{out}^m, n_{in}^m) , from all m previous iterations

$$\begin{aligned} n_{in}^{m+1} &= n_{in}^m - B^1 F^m - \sum_{j=2}^m U^j (V^j)^T F^m \quad (13) \\ F^m &= n_{out}^m - n_{in}^m, \\ U^i &= -B^1 (F^i - F^{i-1}) + n_{in}^i - n_{in}^{i-1} \\ &\quad - \sum_{j=2}^{i-1} U^j (V^j)^T (F^i - F^{i-1}), \\ (V^i)^T &= \frac{(F^i - F^{i-1})^T}{(F^i - F^{i-1})^T (F^i - F^{i-1})}. \end{aligned}$$

The initial guess B^1 is taken to be a small constant ($\sim 0.1 - 0.01$) so that the input to the second iteration is effectively constructed using the simple mixing. The scheme given by Eqs. (13) requires the storage of relatively small number vectors which is thus more effective than the original Broyden's second method.

IV. RESULTS AND DISCUSSION

A. A few electron open dot

We calculate the magnetotransport of a split-gate open quantum with following parameters representative for a typical experimental structure. The 2DEG is buried at $b = 60$ nm below the surface (the widths of the cap, donor and spacer layers are 10 nm, 36 nm and 14 nm respectively), the donor concentration is $0.6 \cdot 10^{24} \text{ m}^{-3}$. The width of the semi-infinite leads is $w_{lead} = 540$ nm, and the width of the constrictions is $w_{qpc} = 100$ nm (both the quantum point contacts are identical), see Fig. 1 (b). The length of the quantum dot is kept constant throughout the paper, $l_{dot} = 160$ nm, while the width of the dot is varied in the range $w_{dot} = 170 - 440$ nm. The gate voltages applied to the gates is $V_{lead} = -0.4$ V and $V_{qpc} = -0.44$ V. With these parameters of the device there are 14 channels available for propagation in the leads and the electron density in the center of the leads is $n_{lead} = 1.6 \cdot 10^{15} \text{ m}^{-2}$. The maximal electron density in the dot (for $w_{dot} = 440$ nm) is also $n_{dot} = 1.6 \cdot 10^{15} \text{ m}^{-2}$. The temperature is fixed at $T = 0.2$ K for all results presented below.

In the following we discuss the open quantum dot with $N = 1$ propagating channel through both quantum point contacts. Note, that increasing the number of propagating channels to $N = 2, 3$ does not qualitatively change the results presented below. In order to set up the QPCs in the one-mode regime, we grounded one of them and studied the conductance of the remaining QPC as a function of the gate voltage V_{qpc} . The calculated conductance shows a characteristic step-like dependence and we choose V_{qpc} at the first conductance plateau, namely, $V_{qpc} = -0.44$ V.

Figure 3 shows the color-scale plot of the conductance G as a function of the dot width w_{dot} and the gate voltage V_g (the magnetic field is restricted to zero). The distinctive feature of the open quantum dots is the oscillations of the conductance, in response to the change of the geometrical size or the Fermi energy. (Various aspects of the conductance oscillations in small and large dots have been the subject of numerous experimental and theoretical works during the last decade¹). In the present study we concentrate on two dots with $w_{dot} = 170$ nm and $w_{dot} = 430$ nm (as indicated by arrows in Fig. 3). As will be shown below, the first dot corresponds to the transport regime when $\Delta \gg \Gamma$, whereas the second dot operates in the regime $\Delta \sim \Gamma$, where $\Delta = \frac{2\pi\hbar^2}{m^*S_a}$ is the mean level spacing separation in the dot with the actual

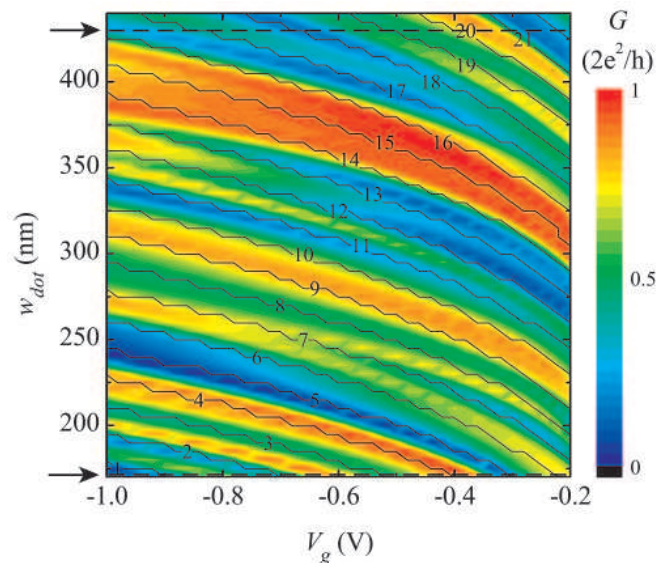


FIG. 3: (color online) The conductance of the open quantum dot as a function of the width, w_{dot} , and the gate voltage V_g calculated within the Hartree approximation. Solid thin lines denote the number of electrons. [Note that a zig-zag-type behavior of the electron number is an artifact due to finite grid steps]. Arrows indicate $w_{dot} = 170$ nm and $w_{dot} = 430$ nm corresponding to two regimes, $\Delta \gg \Gamma$ and $\Delta \sim \Gamma$, discussed in Sec. IV.

area S_a , and Γ is the lead-induced broadening of the resonant energy levels.

It is worth to note that a linear change of the gate voltage leads to a nonlinear change of the effective dot size (If it were linear, the conductance oscillations in Fig. 3 would exhibit a perfect linear-stripe-type pattern). This is consistent with the experimental results of Ref. 30 that show a deviation from the linear dependence of the gate depletion distance as the gate voltage was varied.

B. Regime $\Delta \gg \Gamma$

Figure 4 shows the number of electrons in the few-electron open quantum dot, the conductance and the peak-energy level position as a function of the gate voltage V_g for a quantum dot with $w_{dot} = 170$ nm calculated in the Hartree, DFT and TF approximations (The Hartree approximation corresponds to disregarding of the exchange-correlation potential in Eq. (3), $V_{xc} = 0$). The peak positions of the resonant energy levels in the dot are extracted from the calculated DOS, as illustrated in Fig. 4 (c) for the case when the gate voltage $V_g = -0.6$ V. The estimation of the mean level separation gives $\Delta \approx 0.6$ meV (for $V_g = -0.6$ V) which agrees quite well with the actual level separation shown in Fig. 4 (c) - (e). [Note that within the given interval of variation of V_g , the actual dot area changes and hence Δ varies as well]. An inspection of the DOS shows that the the separation be-

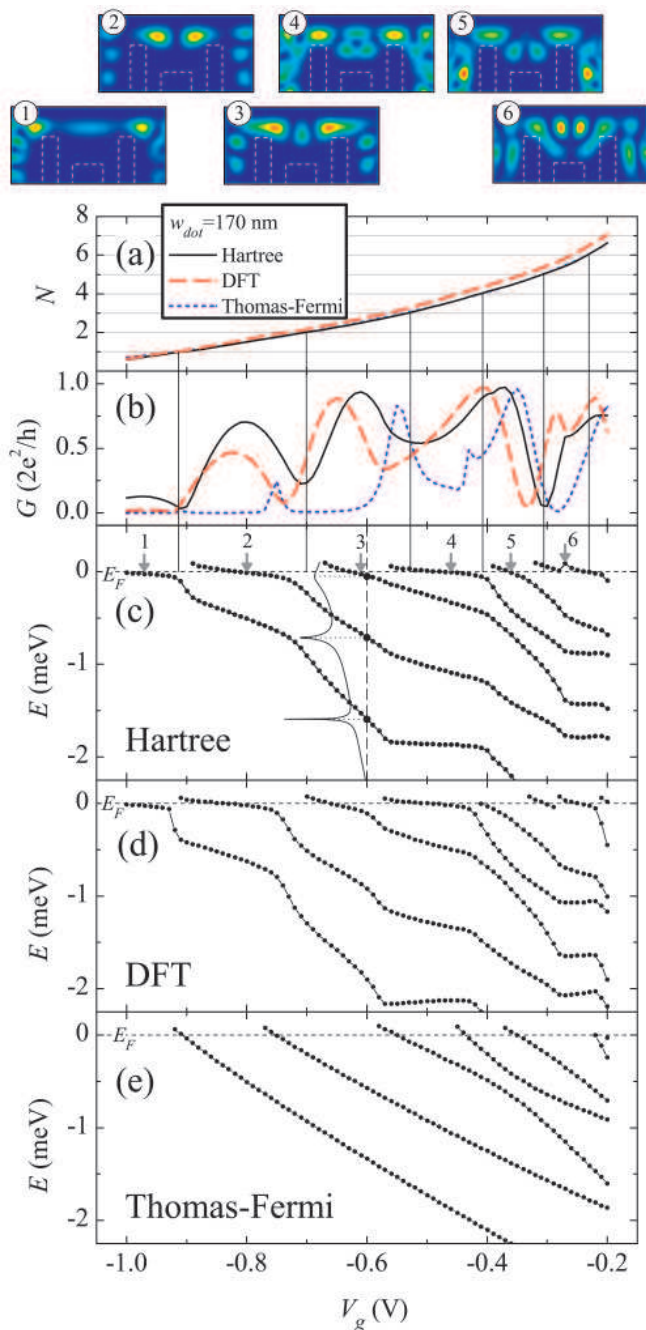


FIG. 4: (color online) (a) The number of electrons, (b) the conductance, and (c)-(e) resonant energy structure in the few-electron open quantum dot with $w_{dot}=170$ nm calculated within the Hartree, DFT and Thomas-Fermi approximations. The top panel shows the electron probability amplitudes $|\Psi(x,y)|^2$ for the resonant energy levels marked by arrows in (c). Inset in (c) shows the DOS for $V_g=-0.6$ V.

tween the resonant levels are much larger than the level broadening, $\Delta \gg \Gamma$.

All three approximations give very similar electron number N in the dot as a function of the gate voltage V_g . N monotonically increases with increase of V_g , which

reflects the fact that electrons freely enter and leave the dot in the open regime. However, the conductance calculated in the Hartree and the DFT approximations exhibit rather similar behavior, whereas the Thomas-Fermi conductance shows a very different gate voltage dependence. The origin of this difference can be understood from the analysis of the resonant level structure. *The resonant energy levels calculated within the Hartree and DFT approximations get pinned to the Fermi energy*, see Figs. 4(c) and (d) respectively. In stark contrast, the energy level positions calculated in the Thomas-Fermi approximation sweep past the Fermi level in a linear fashion when the applied voltage is varied, Fig. 4 (e).

The effect of level pinning is related to the screening properties of the open quantum dot and the presence of the resonant structure in its DOS. Indeed, in the vicinity of the resonances the DOS of the dot is enhanced such that electrons with the energies close to E_F (when $f_{FD} < 1$) can easily screen the external potential. This leads to the metallic behavior of the system when the electron density in the dot can be easily redistributed to keep the potential constant. As a result, in the vicinity of a resonance the system only weakly responds to the external perturbation (change of a gate voltage, magnetic field, etc.), i.e. the resonant levels becomes pinned to the Fermi energy. A comparison between the Hartree and the DFT approximations indicate that the exchange-correlation interaction seems to enhance the pinning, but an overall change is small (c.f. Figs. 4 (c) and (d)). Thus, in the following we concentrate on the Hartree approximation only. In contrast to the Hartree and the DFT approaches, the effect of pinning is absent in the TF approximation. This is because the total confining potential calculated within the TF approximation does not capture the resonant structure of the DOS. Note that a modelling of the magnetotransport in a quantum dot conceptually similar to our TF approach was performed by Bird *et al.*³¹, where the confining potential for every given gate voltage was obtained as a self-consistent solution of the Poisson equation.

Conductance oscillations in the open quantum dots can be related to presence/absence of the resonant energy levels at E_F . Indeed, the first three peaks in the Hartree conductance are attributed to the presence of corresponding resonant levels, which is confirmed by the inspection of the wave function $|\Psi(x,y)|^2$ (by counting the number of nodes of $|\Psi(x,y)|^2$), Fig. 4. In turn, the dips indicate the absence of levels at E_F and agree precisely with integer N reflecting the fact that all the available levels are below E_F and thus are fully filled. Note that for less negative gate voltages ($|V| \lesssim 0.3$ V) the separation between the levels Δ becomes comparable to the broadening Γ , such that the dips in the conductance are no longer correspond to the integer electron number N (see next section for details). It is also interesting to note that the resonant state corresponding to the 5th eigenstate (5 nodes of the $|\Psi(x,y)|^2$) is situated lower in energy than the corresponding resonant state related to the 4th eigen-

state. This is an indication that 5th state couples with the leads more strongly than 4th state³².

The pinning of the resonant energy levels has an important effect on transport in open quantum dots. In the considered transport regime, $\Delta \gg \Gamma$, the conductance calculated within the one-electron (TF) approximation exhibits distinct peaks separated by broad valleys of essentially zero conductance. This reflects the structure of the one-electron DOS where the resonant levels sweep past the Fermi level in a linear fashion. In contrast, as a result of pinning, the DFT and Hartree conductance shows much broader oscillations in comparison to the one-electron approach (Fig. 4(b)).

C. Regime $\Delta \sim \Gamma$

When an effective size of a quantum dot increases, the mean level spacing separation Δ decreases. For the quantum dot of the size $w_{dot} = 430$ the estimation of the mean level separation gives $\Delta \approx 0.15$ meV (for $V_g = -0.6$ V) which agrees quite well with the actual level separation shown in Fig. 5 (c) - (d). An inspection of the DOS shows that for this dot the spacing between neighboring levels is comparable with the level broadening, $\Delta \sim \Gamma$, see Fig. 5(c). [Note, that the level broadening is controlled by coupling to the leads and does not depend on the dot size.] Because neighboring levels start to overlap, there is always one or several energy states at E_F mediating transport through the dot. The effect of the pinning of the energy levels in the Hartree calculations (as well as its absence in the TF calculations) is also clearly seen in this regime as well. However, in contrast to the regime $\Delta \gg \Gamma$, the dips in the conductance can no longer be related to the integer number of electrons in the dot. Instead, it is the interference between states at the entrance and exit of the open quantum that determines the dependence $G = G(V_g)$ ³². Our preliminary results for the conductance of even larger dots (containing hundreds of electrons) outline different features of the TF and Hartree conductances that are manifest themselves in the amplitude and the broadening of the conductance peaks. A detailed analysis of the statistics of the conductance oscillations is however outside the scope of the present work and will be deferred to future publications.

D. Effect of magnetic field

In a sufficiently high magnetic field the electron transport takes place by the edge states with a characteristic dimension of the order of the magnetic length $l_B = \sqrt{\hbar/eB}$. In the edge state transport regime backscattering on the potential defining the quantum dot decreases and, for a large enough B , electrons pass through the device with the transmission close to unity. Transport in such a regime is referred to as adiabatic. For the open quantum dot of $w_{dot} = 430$ nm, transition to adi-

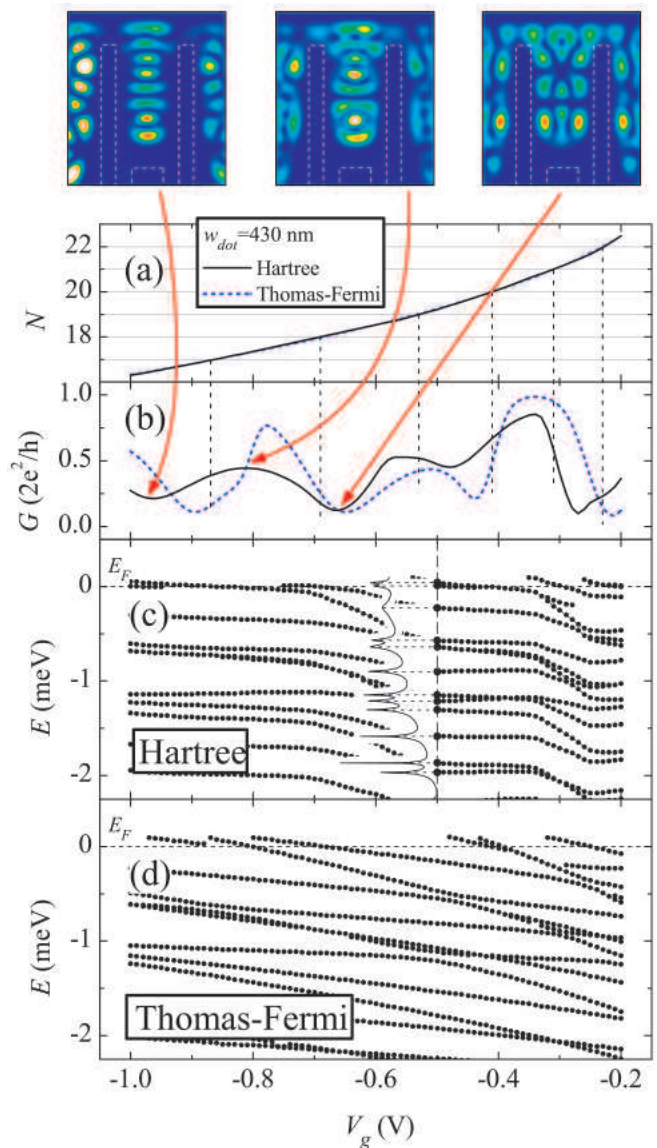


FIG. 5: (color online) (a) The number of electrons, (b) the conductance, and (c)-(d) resonant energy structure in the few-electron open quantum dot with $w_{dot}=430$ nm calculated within the Hartree and Thomas-Fermi approximations. The electron probability amplitudes $|\Psi(x,y)|^2$ are shown for some representative V_g (top panel). Inset in (c) shows the DOS for $V_g=-0.5$ V.

atic propagation takes place at about $B \approx 0.5$ T, see Fig. 6(a). The conductance for $B \gtrsim 0.5$ T shows pronounced oscillations due to the Aharonov-Bohm interference. When the magnetic field changes such that the total magnetic flux $\Phi = BS$ through the dot modifies by the one flux quantum $\phi_0 = h/e$, the conductance demonstrates periodic oscillations with the period $\Delta B = \phi_0/S$ (S is the characteristic area of the dot). Using the actual dot area S_a we get $\Delta B = 0.11$ T, which is nearly twice less than extracted from Fig. 6(a), where $\Delta B = 0.25$ T. The discrepancy can be related to a finite extent of

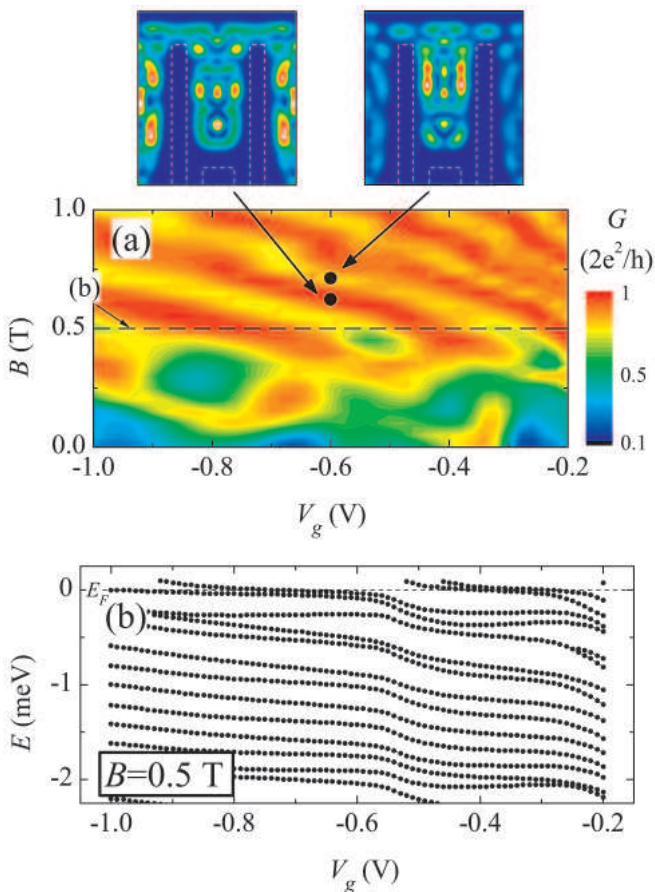


FIG. 6: (color online) (a) The conductance of the open quantum dot as a function of the magnetic field B and gate voltage V_g for the open quantum dot of the width $w_{dot}=430$ nm calculated within the Hartree approximation. (b) The energy structure for $B = 0.5$ T calculated within the Hartree approximation. The top panel shows the electron probability amplitudes $|\Psi(x, y)|^2$ (top) for two representative magnetic fields.

the edge state circulating inside the dot ($l_B \approx 35$ nm for $B = 0.5$). As a result, the area enclosed by the edge state is much smaller than the geometrical area of the dot.

The resonant energy structure is modified substantially when a magnetic field is applied, c.f. Fig. 6(b) for $B = 0.5$ T and Fig. 5 (c) for $B = 0$ T. The resonant levels exhibit almost equal separation which can be related to the well-known Darwin-Fock-type energy spectrum formation for the corresponding closed dot³³. The distinguished feature of the energy level structure is much stronger pinning of the resonant levels to E_F that persists over larger intervals of V_g in comparison to the $B = 0$ case. Stronger pinning can be attributed to the enhanced screening efficiency because of the increased localization of the wave function for the case of nonzero magnetic field. As we mentioned in the introduction the strong pinning of the resonant energy levels in the presence of the magnetic field can have a profound effect on transport properties of various devices operating

in the edge state transport regime including the Mach-Zender¹⁷ and the Laughlin¹⁸ interferometers as well as antidot devices^{19,20,21,22}.

To conclude this section, it is worth mentioning that another manifestation of the screening in the edge state regime is the well-known effect of formation of the compressible and incompressible strips near the structure boundary¹⁰.

E. Open vs closed system

In modelling quantum mechanical transport in quantum dots and related systems one often uses an approximation where an inherently open system is replaced by a corresponding large, but closed one, see e.g.³⁴. In this section we critically examine such an approximation. In particular, we address a question whether a conductance calculated in such a way coincides with the conductance of a truly open system, and whether the pinning of the resonant energy levels is survived or not. For modelling of the closed system, we replace the semi-infinite leads by the potential walls of an infinite height such that the solution of the Schrodinger equation reduces to the eigenproblem

$$H\psi = E\psi, \quad (14)$$

where E and ψ are discrete sets of eigenvalues and eigenvectors, and the Hamiltonian H is given by Eq. (1). We solve Eq. (14) self-consistently performing the fast Fourier transformation from the coordinate into the energy space, which greatly reduces a computational cost.

In our calculations we fix the Fermi energy such that the charge density in the system is given as

$$n(\mathbf{r}) = \sum_i \psi_i(\mathbf{r}) f(E_i - E_F). \quad (15)$$

This assumption leads to a noninteger electron number in a system, but we a priori construct the closed system resembling the open one as much as possible. Note also, that because the total number of electrons $N_{tot} \gg 1$, the effect of the non-integer N_{tot} on the total potential is practically negligible.

In order to calculate the conductance of the system at hand, we cut off slices in the vicinity of the boundaries as illustrated in Fig. 7(a) and then add homogeneous semi-infinite leads with the potential that matches the potential of the boundary slices. Finally, we solve a scattering problem for this given potential using the recursive Greens function technique¹².

Figures 7(b)-(d) show the electron number in the dot N , the conductance G and the resonant energy structure within the Hartree approximation. The comparison to the corresponding results for the open system shows that the closed-system approximation reproduces all the results not only qualitatively but rather quantitatively, c.f. Fig. 4. The only difference is the shift along V_g -axis

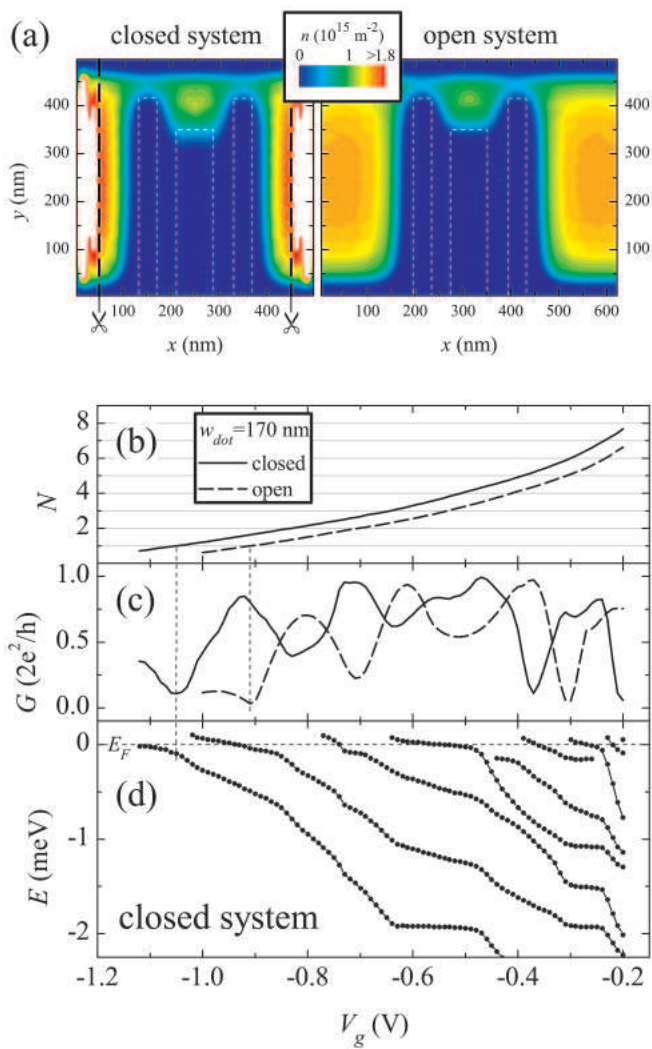


FIG. 7: (color online) (a) The representative self-consistent charge densities for the closed and open systems. The thick dashed lines show the cuts for the transport calculations. (b) The electron number, (c) the conductance and (d) the peak energy-level position calculated within the Hartree approximation in the closed-system approximation. The dashed lines denote the result for the open system (the same as in Fig. 4). The width of the quantum dot is $w_{dot}=170 \text{ nm}$.

which is simply related to the fact that the Hartree potential for the case of the closed system, in contrast to the open one, does not include a contribution from the semi-infinite leads. Figure 7(d) reveals that the pinning of resonant energy levels to the Fermi energy is present in the closed system-approximation as well. We thus conclude that this approximation might be used for the modelling of the transport properties and the resonant energy level structure of the corresponding open system. We however should note that with the present approximation we could not satisfy the convergence criterium (12) that we routinely use for the calculation of the conductance in the open systems as described in Sec. III.

V. CONCLUSION

We have developed an approach for full quantum mechanical many-body magnetotransport calculations in open systems that starts from the lithographical layout of the device and does not include phenomenological parameters like coupling strengths, charging constants etc. The whole device, including semi-infinite leads, is treated on the same footing (i.e. the electron-electron interaction is accounted for in both the leads as well as in the dot region). The many-body effects are included within the DFT and the Hartree approximations.

The developed method was applied to calculate the conductance through an open quantum dot. The main finding of the present paper is the effect of pinning of the resonant levels to the Fermi energy due to the enhanced screening. Our results represent a significant departure from a conventional picture where a variation of external parameters (such as a gate voltage, magnetic field, etc.) causes the successive dot states to sweep past the Fermi level in a linear fashion. We instead demonstrate highly nonlinear behavior of the resonant levels in the vicinity of the Fermi energy. We show that the pinning effect is absent in a one-electron (Thomas-Fermi) approximation because in this case the self-consistent potential does not account for the resonant structure of the DOS in the dot. The pinning of the resonant levels in open quantum dots leads to the broadening of the conduction oscillations in comparison to the one electron picture. It remains to be seen whether accounting for this effect might shed new light on the interpretation of the conductance oscillation statistics in open quantum dots.

The pinning of the resonant levels becomes much more pronounced in the presence of the perpendicular magnetic field. This can be attributed to the enhanced screening efficiency because of the increased localization of the wave function. The strong pinning of the resonant energy levels in the presence of magnetic field can have a profound effect on transport properties of various devices operating in the edge state transport regime including Mach-Zender¹⁷ and Laughlin¹⁸ interferometers as well as antidot devices^{19,20,21,22}.

We should stress that the pinning effect predicted in this paper is not specific to the considered material system (GaAs/AlGaAs heterostructure) and is expected to hold in any two-dimensional system in open transport regime (e.g. Si inversion layer structures, etc.).

Finally, in the present paper we critically examined an approximation used in modelling of quantum mechanical transport in quantum dots and related systems when an inherently open system is replaced by a corresponding large, but closed one.

In the present study we have limited ourselves to the case of spinless electrons. Work is in progress to include the effect of the spin in order to revisit the effect of spin splitting recently observed in open quantum dots^{9,28}.

Acknowledgments

S. I. acknowledges financial support from the Swedish Institute and the EU network SINANO. Numerical cal-

culations were performed in part using the facilities of the National Supercomputer Center, Linköping, Sweden.

-
- ¹ For a review, see, e.g., C. W. J. Beenakker, *Rev. Mod. Phys.* **69**, 731 (1997); Y. Alhassid, *Rev. Mod. Phys.* **72**, 895 (2000).
- ² S. Datta, *Nanotechnology* **15**, S433 (2004).
- ³ For a review, see, e.g., M. Kastner, *Ann. Phys. (Leipzig)* **9**, 885 (2000).
- ⁴ M. Ciorga, A. S. Sachrajda, P. Hawrylak, C. Gould, P. Zawadzki, S. Jullian, Y. Feng, and Z. Wasilewski, *Phys. Rev. B* **61**, R16315 (2000).
- ⁵ I. V. Zozoulenko, A. S. Sachrajda, C. Gould, K.-F. Berggren, P. Zawadzki, Y. Feng, and Z. Wasilewski, *Phys. Rev. Lett.* **83**, 1838 (1999).
- ⁶ T. K. Ng and P. A. Lee, *Phys. Rev. Lett.* **61**, 1768 (1988); L. I. Glazman and M. E. Raikh, *JETP Lett.* **47**, 452 (1988).
- ⁷ L. E. Henrikson, A. J. Glick, G. W. Bryant, D. F. Barbe, *Phys. Rev. B* **50**, 4482 (1994).
- ⁸ K. M. Indlekofer, J. P. Bird, R. Akis, D. K. Ferry and S. M. Goodnick, *J. Phys.: Condens. Matter* **15**, 147(2003) .
- ⁹ M. Evaldsson, I. V. Zozoulenko, M. Ciorga, P. Zawadzki, and A. S. Sachrajda, *Europhys. Lett.* **68**, 261 (2004).
- ¹⁰ D. B. Chklovskii, B. I. Shklovskii, and L. I. Glazman, *Phys. Rev. B* **46**, 4026 (1992).
- ¹¹ For a review, see, e.g., S. M. Reimann and M. Manninen, *Rev. Mod. Phys.* **74**, 1283 (2002).
- ¹² I. V. Zozoulenko, F. A. Maaø and E. H. Hauge, *Phys. Rev.* **53**, 7975 (1996); *Phys. Rev.* **53**, 7987 (1996); *Phys. Rev.* **56**, 4710 (1997).
- ¹³ B. Tanatar and D. M. Ceperley, *Phys. Rev. B* **39**, 5005, (1989).
- ¹⁴ R. G. Parr and W. Yang, *Density-Functional Theory of Atoms and Molecules*, (Oxford Science Publications, Oxford, 1989).
- ¹⁵ see e.g., H. Saarikoski, E. Räsänen, S. Siljamäki, A. Harju, M. J. Puska, and R. M. Nieminen, *Phys. Rev. B* **67**, 205327 (2003).
- ¹⁶ I. P. Radu, J. B. Miller, S. Amasha, E. Levenson-Falk, D. M. Zumbuhl, M. A. Kastner, C. M. Marcus, L. N. Pfeiffer, and K. W. West, to be submitted to *Phys. Rev. B*; S. Ihnatsenka and I. V. Zozoulenko, to be submitted to *Phys. Rev. B*.
- ¹⁷ Y. Ji, Y. Chung, D. Sprinzak, M. Heiblum, D. Mahalu, and H. Shtrikman, *Nature* **422**, 415 (2003).
- ¹⁸ F. E. Camino, W. Zhou, and V. J. Goldman, *Phys. Rev. B* **72**, 075342 (2005).
- ¹⁹ see e. g., S. Das Sarma, M. Freedman, and C. Nayak, *Phys. Today* **59** (7), 32 (2006), and references therein.
- ²⁰ C. J. B. Ford, P. J. Simpson, I. Zailer, D. R. Mace, M. Yosefin, M. Pepper, D. A. Ritchie, J. E. F. Frost, M. P. Grimshaw, and G. A. C. Jones, *Phys. Rev. B* **49**, 17456 (1994); M. Kataoka, C. J. B. Ford, G. Faini, D. Maily, M. Y. Simmons, and D. A. Ritchie, *Phys. Rev. B* **62**, R4817 (2000).
- ²¹ I. Karakurt, V. J. Goldman, J. Liu, and A. Zaslavsky, *Phys. Rev. Lett.* **87**, 146801 (2001); M. Kataoka and C. J. B. Ford, *Phys. Rev. Lett.* **92**, 199703 (2004); V. J. Goldman, *Phys. Rev. Lett.* **92**, 199704 (2004); S. Ihnatsenka and I. V. Zozoulenko, *Phys. Rev. B* **74**, 201303(R) (2006).
- ²² I. V. Zozoulenko and M. Evaldsson, *Appl. Phys. Lett.* **85**, 3136 (2004).
- ²³ J. H. Davies, I. A. Larkin, and E. V. Sukhorukov, *J. Appl. Phys.* **77**, 4504 (1995).
- ²⁴ J. Martorell, H. Wu, and D. W. L. Sprung, *Phys. Rev. B* **50**, 17298 (1994).
- ²⁵ S. Datta, *Electronic Transport in Mesoscopic Systems*, (Cambridge University Press, Cambridge, 1997).
- ²⁶ S. Ihnatsenka and I. V. Zozoulenko, *Phys. Rev. B* **73**, 075331 (2006); S. Ihnatsenka and I. V. Zozoulenko, *Phys. Rev. B* **73**, 155314 (2006).
- ²⁷ Y. Wang, J. Wang, H. Guo, and E. Zaremba, *Phys. Rev. B* **52**, 2738 (1995).
- ²⁸ M. Evaldsson and I. V. Zozoulenko, *Phys. Rev. B* **73**, 035319 (2006).
- ²⁹ D. Singh, H. Krakauer, and C. S. Wang, *Phys. Rev. B* **34**, 8391 (1986).
- ³⁰ I. V. Zozoulenko, A. S. Sachrajda, P. Zawadzki, K.-F. Berggren, Y. Feng and Z. Wasilewski, *Phys. Rev. B* **58**, 10 597 (1998).
- ³¹ J. P. Bird, R. Akis, D. K. Ferry, D. Vasileska, J. Cooper, Y. Aoyagi, and T. Sugano, *Phys. Rev. Lett.* **82**, 4691 (1999).
- ³² I. V. Zozoulenko and K.-F. Berggren, *Phys. Rev. B* **56**, 6931 (1997).
- ³³ J. Davies, *The Physics of Low-Dimensional Semiconductors*, (Cambridge University Press, Cambridge, 1998).
- ³⁴ D. Jovanovic and J.-P. Leburton, *Phys. Rev. B* **49**, 7474 (1994).